

Physics performance of the STAR zero degree calorimeter at relativistic heavy ion collider

Yi-Fei Xu^{1,2} · Jin-Hui Chen¹ · Yu-Gang Ma^{1,3} ·
Ai-Hong Tang⁴ · Zhang-Bu Xu⁴ · Yu-Hui Zhu^{1,2}

Received: 19 May 2016/Revised: 5 August 2016/Accepted: 12 August 2016/Published online: 17 September 2016
© Shanghai Institute of Applied Physics, Chinese Academy of Sciences, Chinese Nuclear Society, Science Press China and Springer Science+Business Media Singapore 2016

Abstract The zero degree calorimeter (ZDC) at RHIC-STAR was installed in the year 2000. After running for more than 10 years, the performance of the STAR-ZDC cannot maintain a proper status because of the radiation damage. The ZDC on RHIC-BRAHMS had been moved to STAR in 2011 after some tests. We present here the result of the tests as well as the physical performance of those ZDC modules between the 2011 and 2015 RHIC runs. The excellent energy resolution of the ZDC in heavy ion collision provides a good candidate for future detector development, such as the CSR experiment at CAS-Lanzhou facility.

Keywords Zero degree calorimeter · Calibration · Energy resolution · STAR

This work was supported by the Major State Basic Research Development Program in China (2014CB845400), and the National Natural Science Foundation of China (Nos. 11421505, 11520101004, 11322547, and 11275250).

✉ Yu-Gang Ma
ygma@sinap.ac.cn

Jin-Hui Chen
chenjinhui@sinap.ac.cn

¹ Shanghai Institute of Applied Physics, Chinese Academy of Sciences, Shanghai 201800, China

² University of Chinese Academy of Sciences, Beijing 100049, China

³ ShanghaiTech University, Shanghai 200031, China

⁴ Brookhaven National Laboratory, Upton, NY 11973, USA

1 Introduction

The zero degree calorimeter (ZDC) at the Solenoidal Tracker at RHIC (STAR) are the hadron calorimeter which are installed on both the east and west sides of STAR. The purpose of STAR-ZDC was to detect neutrons emitted from the interaction region and went along the beam direction with a divergence angle less than 4 mrad [1], and measure their total energy. From the measured total energy, one can calculate the multiplicity. The neutron multiplicity is known to be correlated with the event geometry and is used to measure the reaction centrality in mutual beam interactions [1]. The ZDC coincidence of the two beam directions is a minimal bias selection of heavy ion collisions; thus, it is useful as an event trigger and a luminosity monitor [1, 2]. The STAR-ZDC has six identical modules in total, three of them are installed in the east side of the STAR interaction region and three are on the west. We also have shower maximum detector (ZDC-SMD) installed on both sides which provide the position information of the neutron beam. The ZDC-SMD combined detector was used extensively in data analysis for reaction plane determination, such as the charged particle directed and elliptic flow measurement [3–8].

As can be seen in Fig. 1 [1], the ZDC modules consist of tungsten plates, fibers, and photon multiplier tubes. And the ZDCs are installed about 18 m away from the intersection point along the beam line, behind the dipole magnets. The magnets will bend all charged particles and leave the neutrons and other neutral particles to hit the ZDC modules. More detailed technical information about ZDC could be found in Ref. [1].

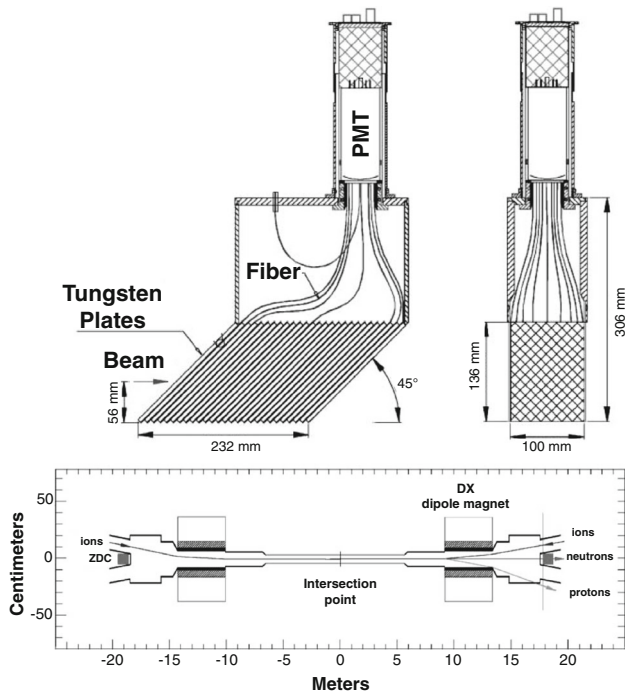


Fig. 1 ZDC structure and plane view of intersection region, dipole magnets, and ZDCs installed. This figure is from Ref. [1]



Fig. 2 ZDC modules installed on RHIC-STAR experiment

2 Test of ZDC gain versus high voltage

The current STAR-ZDC modules are moved from the RHIC-BRAHMS experiment, which were idled since 2006. Before these modules were installed, we tested the relation of ZDC gains versus high voltage applied. Figure 2 shows the ZDC modules on RHIC-STAR experiment.

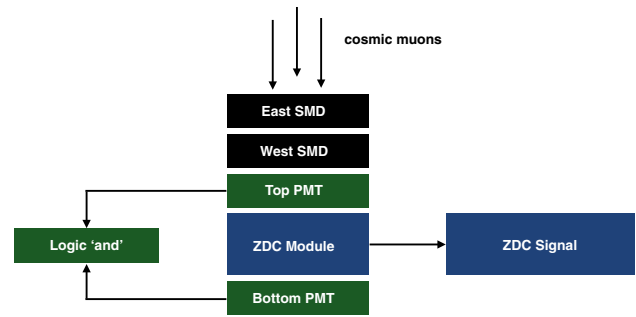


Fig. 3 Electronics layout of the ZDC gain test under different HVs

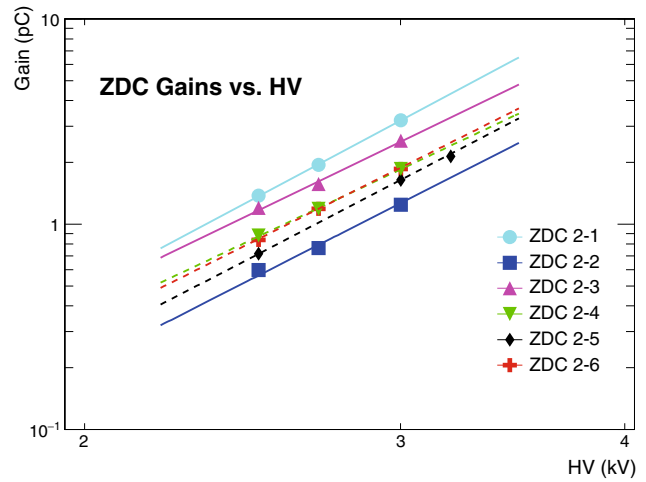


Fig. 4 ZDC gains test under different HVs. The ZDCs 2-1, 2-2, and 2-3 are east modules, and other three are west modules. (Color figure online)

2.1 Electronics layout and general procedure

In order to test the ZDC gain under different high voltages, we constructed an electronics layout as shown in Fig. 3.

Muons from cosmic rays hit sequentially the five modules: the east SMD, the west SMD, the top trigger scintillator, the ZDC module, and the bottom trigger scintillator. Since there are background particles everywhere at anytime, it is essential to use the logic “and” result of the top and bottom scintillators to select events triggered by cosmic ray muons. When a muon hits the ZDC after traversing the top scintillator, it will produce Cherenkov light. The light is guided by the optical fibers and generates a signal in the ZDC. The muon will then hit the bottom scintillator and also generate a signal. The coincidence of the top and bottom scintillator signals is used as the system trigger and provides a gate to the ADC.

Table 1 Fit parameters in test of ZDC gains versus high voltage

Module	a	b
2-1	0.0191 ± 0.0014	4.6616 ± 0.0676
2-2	0.0095 ± 0.0006	4.4533 ± 0.0480
2-3	0.0243 ± 0.0094	4.2267 ± 0.3787
2-4	0.0198 ± 0.0075	4.1288 ± 0.3778
2-5	0.0111 ± 0.0039	4.5443 ± 0.3384
2-6	0.0153 ± 0.0086	4.3839 ± 0.5660

Table 2 Basic information of runs that are used in this article

Run number	Year	Energy ($\sqrt{s_{NN}}$)	Beam type
12130083	2011	200 GeV	Au+Au
15067001	2014	15 GeV	Au+Au
15186001	2014	200 GeV	$^3\text{He}+\text{Au}$
15122044	2014	200 GeV	Au+Au
16134022	2015	200 GeV	p+Au

2.2 Result

The expected relation of PMT module gain with high voltage should be a power law: $\text{gain} = a \times \text{HV}^b$, where a and b are parameters related to the PMT module and environment, and the gain is in unit of pC and voltage is in unit of kV. Ideally, b is related only to the PMT, so as long as we are using PMT modules of the same standard, b should not vary much. The gain versus HV plots of

different ZDCs, and the fitting results, are shown in Fig. 4. The fit parameters are listed in Table 1.

2.3 Conclusion

As we can see from the result shown in Fig. 4, different fit lines are nearly parallel to each other, which is reasonable since the slope b is a PMT-related parameter and it should have nearly the same value. From the relation between the gain and high voltage, we can get separate values of high voltages necessary for different ZDCs to have the same gain.

3 Experimental performance

After installed into STAR, the ZDC modules encountered different beam types in different energies. Here we collect five different runs, as shown in Table 2, to show the ZDC tower gain ratios and the single neutron peak distributions. We then will discuss both the high voltage calibration of ZDC by investigating the gain ratios and the energy resolution by plotting single neutron peaks. The basic information of those runs is listed in Table 2.

3.1 Tower gains and high voltage applied

When a neutron flies through three ZDC modules, the gain in each tower decreases from the first tower to the last

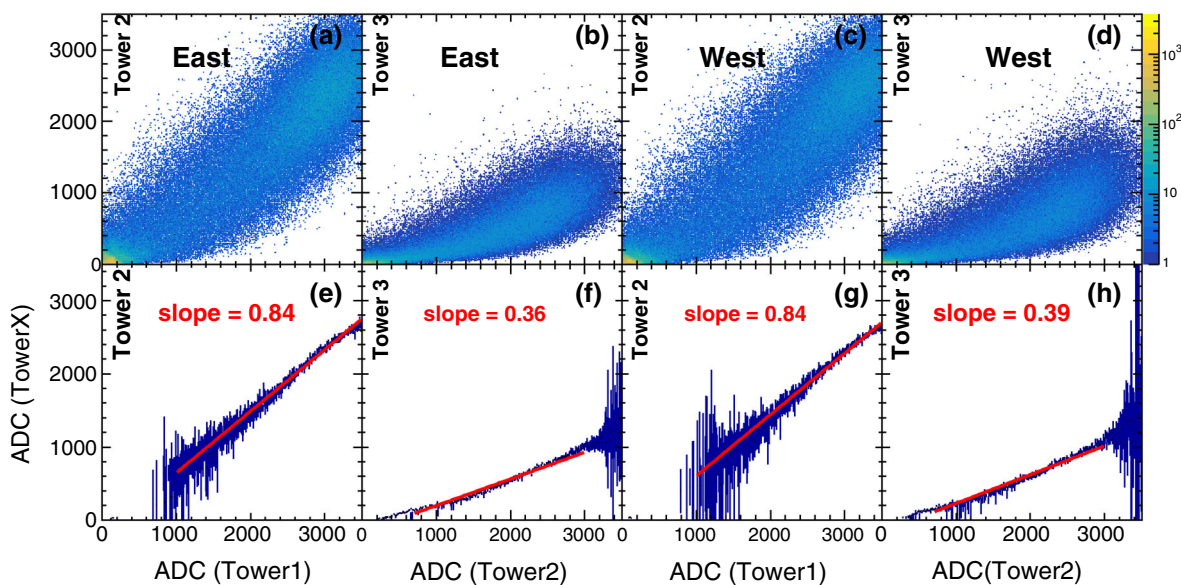


Fig. 5 Tower gains distribution of run 12130083 (Au+Au @ 200 GeV). **a, b, e, and f** are east towers; **c, d, g, and h** are west towers. The upper four panels show the gains distribution between tower1/2 and tower 2/3. The mean gain ratios versus ADC are then

shown in the four lower panels. The red straight line is a linear fit; the slope indicates the gain ratio between two towers. (Color figure online)

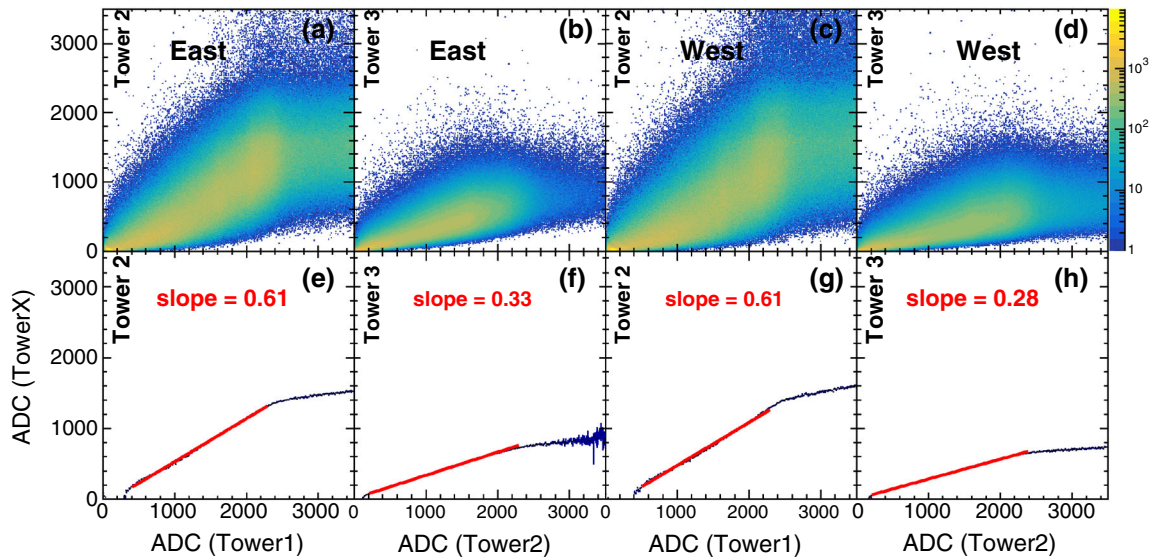


Fig. 6 Tower gains distribution of run 15122044 (Au+Au @ 200 GeV). (Color figure online)

one due to the energy loss in ZDC material. Ideally, the ratio of ZDC tower gains should roughly be 6:3:1. However, it is difficult to tune the high voltage perfectly in practice as the gains will be affected by many factors like beam conditions and shower leakage. So in this article, we consider the HV setting to be good if the ratios are not far from the ideal value. With the runs listed in Table 2, we will show the ratios with different beam types in Figs. 5, 6, and 7.

For Au+Au runs at $\sqrt{s_{NN}} = 200$ GeV in the year 2011, as shown in Fig. 5, the gain ratios between tower 1&2 and 2&3 for both sides are shown in four upper panels. The mean gain ratios versus ADC are then shown in the four lower panels. The slope of a linear fit will indicate the ratio between towers. The uncertainties of the slopes are always on the order of 10^{-3} , so they are not shown. The fitting range varies from plot to plot, because, in the low- x range, the small signal may introduce large errors, and in the high- x range, the shower leakage and other effects will break the linear relation. Figure 5 shows that, on east side, the slope for tower2/tower1 is 0.84 and for tower3/tower2 is 0.36. For west side, the slopes are 0.84 and 0.39 for tower2/tower1 and tower3/tower2, respectively.

For Au+Au runs at $\sqrt{s_{NN}} = 15$ GeV in the year 2014, the neutrons emitted from the peripheral collisions will not carry much energy at this low energy. So it is not possible to obtain the slopes as we did for the run above due to the small gains on towers. We counted the raw gains for each tower and calculated the ratio directly between towers: The ratio is 6.38:1.61:1 on the east, and is 7.35:2.37:1 on the west, where we take the gain of third tower as unit of 1.

For Au+Au runs at $\sqrt{s_{NN}} = 200$ GeV in the year 2014, we still plot the gains and the slopes between towers as

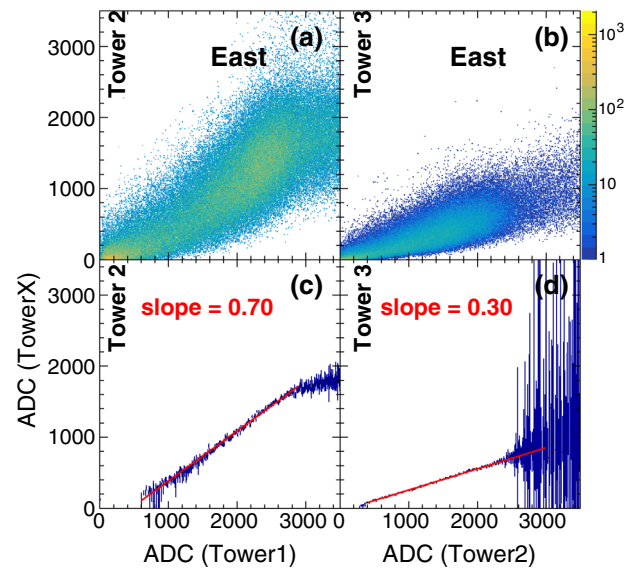


Fig. 7 Tower gains distribution of run 15186001 ($^3\text{He}+\text{Au}$ @ 200 GeV). All four panels are for east side. (Color figure online)

shown in Fig. 6. In the figure, the slopes for tower2/tower1 and tower3/tower2 are 0.61 and 0.33 for east side, and for west side they are 0.61 and 0.28.

We also have $^3\text{He}+\text{Au}$ runs at $\sqrt{s_{NN}} = 200$ GeV in the year 2014. In this run, we have asymmetric beam types, which is quite different from runs above. After collisions, the neutral residual of the gold ions will hit the east ZDC modules, while the residual of ^3He will hit the west modules. The ZDC gains are quite different from east to west. The gold ions contain more neutrons, so the east ZDC gains are larger than west. In Fig. 7, we show the ZDC gains and the slopes, the west side is not shown due to the low ZDC

Fig. 8 Single neutron peak from run 12130083 (AuAu@200 GeV). **a** From the east side, and **b** from the west side. The black lines in both panels are Gaussian fittings. The fitting parameters are also shown in the panels. (Color figure online)

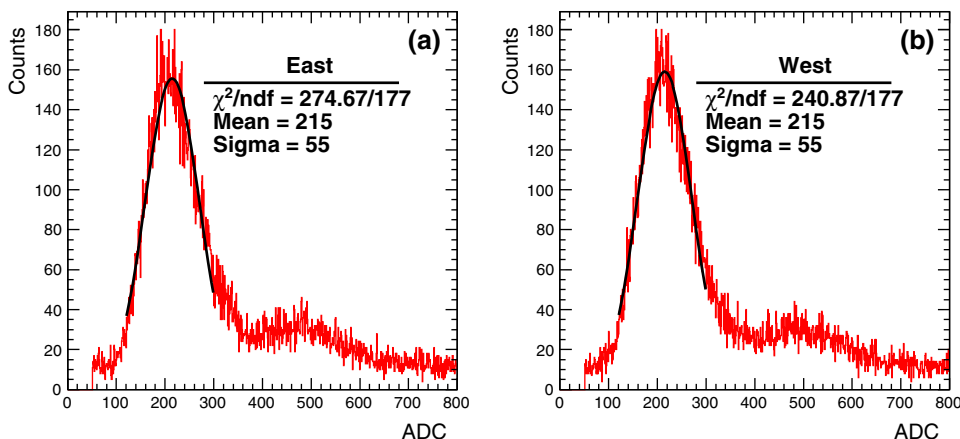
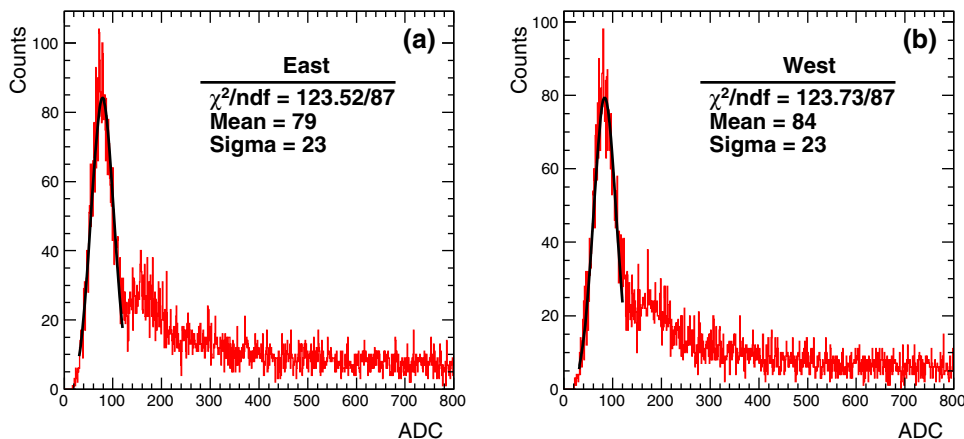


Fig. 9 Single neutron peak from run 15122044 (Au+Au @ 200 GeV). (Color figure online)



gains. From the figure, we can see that the slope of tower2/tower1 is 0.70, while that of tower3/tower2 is 0.30.

For p+Au runs at $\sqrt{s_{NN}} = 200$ GeV in the year 2015, the beam types are also asymmetric. From the raw gains, the ratio between towers is 6.88:3.10:1 on the east side and 9.80:2.75:1 on the west side.

As mentioned above, it is quite difficult to tune the high voltages to get ideal gain ratios. In this article, by fitting, or by direct use of raw gains, we evaluate the HV settings by calculating the gain ratios of towers. Considering that the tower gains are affected by many factors, we think those HV settings are acceptable.

3.2 Energy resolution

The single neutron peak from peripheral collisions is used to determine the energy resolution of the ZDC. The energy resolution of ZDC modules has been simulated and tested in a test beam before. In those tests, the resolution is around $\sigma_E/E = 20\%$ at $E_n = 100$ GeV [1]. In this section, we will show energy resolution of ZDC in different beam types and energies since 2011. We require a very low time-of-flight detector multiplicity (less than 2) in order to select

the peripheral collisions. We also require the TDC value to be within [500, 2500] in order to reduce the background.

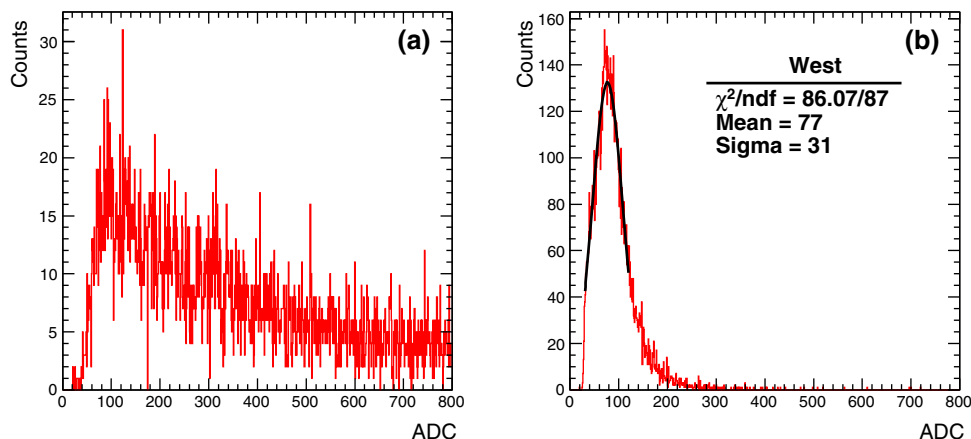
For Au+Au runs at $\sqrt{s_{NN}} = 200$ GeV in 2011, the single neutron peak is shown in Fig. 8. In this figure, the panel (a) is the single neutron peak for the east side ZDC and panel (b) is for the west side ZDC. A Gaussian function was used to fit the peak, and the fitting parameters are shown also in the plot. For both east and west side ZDCs, $\sigma_E/E = 26\%$.

For Au+Au runs at $\sqrt{s_{NN}} = 15$ GeV in 2014, the single neutron peak can hardly be extracted due to the low beam energy.

As shown in Fig. 9, we can see that on east side, $\sigma_E/E = 29\%$, and on west side, $\sigma_E/E = 27\%$. For Au+Au runs at $\sqrt{s_{NN}} = 200$ GeV in 2014, this is consistent with results from the year 2011 run and the early beam test.

In $^3\text{He}+\text{Au}$ runs at $\sqrt{s_{NN}} = 200$ GeV in the year 2014, ^3He is formed by one neutron and two protons, so it is rare to have multiple neutrons hit the west ZDC modules in one collision. This is why we can see a relatively clean single neutron peak on the west side (Fig. 10b). On the east, the peak is not as well as the east one due to high background (Fig. 10a). From the Gaussian fit, on the west,

Fig. 10 Single neutron peak from run 15186001 ($^3\text{He}+\text{Au}$ @ 200 GeV). (Color figure online)



$\sigma_E/E = 40\%$. This σ_E/E is much larger than the same year and the year 2011 Au+Au collisions results. This may be related to the larger beam–beam crossing angle in $^3\text{He}+\text{Au}$ runs than in Au+Au runs.

In p+Au runs at $\sqrt{s_{\text{NN}}} = 200$ GeV in the year 2015, it is rare to have neutrons hit on the west side of ZDC modules since the projectile (proton) contains no neutron. And the gold side, like $^3\text{He}+\text{Au}$ runs, has large background. The single neutron peak cannot be seen on either side.

3.3 Conclusion

We report the beam test and physics performance of the new installed ZDC in STAR experiment since 2011. With the detail runs listed in Table 2, the ZDC gains between towers were obtained and the ratios between towers were calculated. The ratios in these runs are close to expectation, which indicate that the high voltage applied on these modules are acceptable. We are further studying the single neutron peak for those runs. The energy resolutions are reasonably good, although they are a little larger than the early simulation and beam test (from 20 to 27 %) at the year 2000 [1]. We also observed that the energy resolution in $^3\text{He} + \text{Au}$ collisions is not as good as the result in Au+Au collisions, which may be due to larger crossing angle in ^3He (or p) + Au collisions. Our study provides good reference for detector system built-up in the future CSR external target experiment at IMP-CAS facility [9–12].

Acknowledgments We thank the STAR collaboration, the RHIC Operations Group, the Collider-Accelerator Department, and the RHIC Computing Facility at BNL.

References

1. C. Adler, A. Denisov, E. Garcia et al., The RHIC zero degree calorimeters. *Nucl. Instrum. Methods A* **470**, 488–499 (2008). doi:[10.1016/S0168-9002\(01\)00627-1](https://doi.org/10.1016/S0168-9002(01)00627-1)
2. A.J. Baltz, C. Chasman, S.N. White, Correlated forward–backward dissociation and neutron spectra as a luminosity monitor in heavy-ion colliders. *Nucl. Instrum. Methods A* **417**, 1–8 (1998). doi:[10.1016/S0168-9002\(98\)00575-0](https://doi.org/10.1016/S0168-9002(98)00575-0)
3. I. Arsene, I.G. Bearden, D. Beavis et al., Quark-gluon plasma and color glass condensate at RHIC? The perspective from the BRAHMS experiment. *Nucl. Phys. A* **757**, 1–27 (2005). doi:[10.1016/j.nuclphysa.2005.02.130](https://doi.org/10.1016/j.nuclphysa.2005.02.130)
4. B.B. Back, M.D. Baker, M. Ballintijn et al., The PHOBOS perspective on discoveries at RHIC. *Nucl. Phys. A* **757**, 28–101 (2005). doi:[10.1016/j.nuclphysa.2005.03.084](https://doi.org/10.1016/j.nuclphysa.2005.03.084)
5. J. Adams, M.M. Aggarwal, Z. Ahammed et al., Experimental and theoretical challenges in the search for the quark-gluon plasma: The STAR Collaboration’s critical assessment of the evidence from RHIC collisions. *Nucl. Phys. A* **757**, 102–183 (2005). doi:[10.1016/j.nuclphysa.2005.03.085](https://doi.org/10.1016/j.nuclphysa.2005.03.085)
6. K. Adcox, S.S. Adler, S. Afanasiev et al., Formation of dense partonic matter in relativistic nucleus–nucleus collisions at RHIC: experimental evaluation by the PHENIX collaboration. *Nucl. Phys. A* **757**, 184–283 (2005). doi:[10.1016/j.nuclphysa.2005.03.086](https://doi.org/10.1016/j.nuclphysa.2005.03.086)
7. L. Adamczyk, J.K. Adkins, G. Agakishiev et al., Azimuthal anisotropy in U+U and Au+Au collisions at RHIC. *Phys. Rev. Lett.* **115**, 222301 (2015). doi:[10.1103/PhysRevLett.115.222301](https://doi.org/10.1103/PhysRevLett.115.222301)
8. J.H. Chen, Y.G. Ma, G.L. Ma et al., Elliptic flow of ϕ mesons and strange quark collectivity. *Phys. Rev. C* **74**, 064902 (2006). doi:[10.1103/PhysRevC.74.064902](https://doi.org/10.1103/PhysRevC.74.064902)
9. S. Zhang, J.H. Chen, Y.G. Ma et al., Hypertriton and light nuclei production at Λ -production subthreshold energy in heavy-ion collisions. *Chin. Phys. C* **35**(8), 741 (2011). doi:[10.1088/1674-1137/35/8/008](https://doi.org/10.1088/1674-1137/35/8/008)
10. X.D. Yang, J. Li, L.J. Mao et al., Commissioning of electron cooling in CSRm. *Chin. Phys. C (HEP & NP)* **33**, 18 (2009). doi:[10.1088/1674-1137/33/S2/005](https://doi.org/10.1088/1674-1137/33/S2/005)
11. L.G. Chen, J. Gong, K. Wang et al., Variance analysis for passive neutron multiplicity counting. *Nucl. Sci. Tech.* **26**, 020402 (2015). doi:[10.13538/j.1001-8042/nst.26.020402](https://doi.org/10.13538/j.1001-8042/nst.26.020402)
12. S. Zhang, Z.Q. Chen, R. Han et al., Neutron time-of-flight spectrometer based on HIRFL for studies of spallation reactions related to ADS project. *Nucl. Sci. Tech.* **26**, 030502 (2015). doi:[10.13538/j.1001-8042/nst.26.030502](https://doi.org/10.13538/j.1001-8042/nst.26.030502)